ALCHEMY Jurnal Penelitian Kimia

Official Website: https://jurnal.uns.ac.id/alchemy

ISSN 1412-4092
EISSN 2443-4183

Synthesis, Characterization, Hirshfeld Surface Analysis, and Antibacterial Properties of Complex [Ni(4-aminopyridine)$_4$Cl$_2$].H$_2$O

Putri Dwi Lestari, Nani Farida, Husni Wahyu Wijaya, I Wayan Dasna*

Department of Chemistry, Faculty of Mathematics and Natural Sciences, State University of Malang
Jalan Semarang No. 5, Kota Malang, East Java 65145, Indonesia

**Corresponding author: idasna@um.ac.id*

DOI: 10.20961/alchemy.22.2.112417.492-503

Received 10 December 2025, Revised 21 April 2026, Accepted 29 August 2026, Published 30 September 2026

Keywords:

4-aminopyridine; antibacterial agent crystal structure; Ni(II) complex; solvothermal.

ABSTRACT. The reaction between NiCl$_2$·H$_2$O and 4-aminopyridine (4-NH$_2$py) in methanol solvent with a molar ratio of 1:4 successfully produced [Ni(4-aminopyridine)$_4$Cl$_2$]·H$_2$O complex crystallized as blue block-shaped crystals. The single crystal was synthesized using a solvothermal method at 68 °C for 15 hours. The crystal was characterized by melting point determination, Fourier Transform Infrared (FTIR) spectroscopy, molar conductance measurement, and single-crystal X-ray diffraction (SC-XRD) analysis. The complex [Ni(4-NH$_2$py)$_4$Cl$_2$]·H$_2$O is a monomeric complex with a distorted octahedral geometry. The central Ni(II) ion is coordinated by four 4-NH$_2$py ligands through the pyridine nitrogen atoms and two chloride anions, while one H$_2$O molecule is located outside the coordination sphere. The complex crystallizes in a monoclinic lattice system with space group $P2_1/n$ (a = 9.7665(4) Å, b = 17.5841(7) Å, c = 14.0100(6) Å, α = γ = 90°, β = 92.085(2)°) with an R-value of 0.0459. Intermolecular N–H···Cl and H···O interactions are found to be dominant in the structure based on hirshfeld surface analysis. The antibacterial activity of the complex shows higher effectiveness against *Escherichia coli* (9.18 mm) than Staphylococcus aureus (7.99 mm), representing Gram-negative and Gram-positive bacteria, respectively.

INTRODUCTION

N-heterocyclic compounds have long been investigated due to their wide range of applications, including in pharmaceuticals, corrosion inhibitors, dyes, developers, catalysts, and others. These compounds are capable of mimicking various endogenous metabolites, making them important in modern drug development (Amin *et al.*, 2022). Among six-membered N-heterocyclic compounds, aminopyridines have attracted particular attention because of their pharmacological activities. The presence of aminopyridine units in small amounts within a drug molecule, whether simple or complex, can enhance its biological properties (Orie *et al.*, 2021). Furthermore, the formation of metal–aminopyridine complexes can enhance antibacterial activity through interactions between the –NH$_2$ groups and bacterial cell membranes via hydrogen bonding and hydrophobic interactions (Wijaya *et al.*, 2024).

Aminopyridine (C$_5$H$_6$N$_2$) is one of the six-membered heterocyclic compounds containing an amino group and an aromatic heterocyclic pyridine ring. This compound exists in three isomeric forms, namely 2-aminopyridine, 3-aminopyridine, and 4-aminopyridine (Orie *et al.*, 2021). The x-NH$_2$py ligand generally acts as a monodentate ligand through the nitrogen atom of the pyridine ring, as observed in the complexes [Co(2-NH$_2$py)$_2$(dca)$_2$] and [Cu(4-NH$_2$py)$_4$]Cl$_2$·2CH$_3$OH (Ivanova and Mayer-Figge, 2005; Munadhiroh *et al.*, 2022). However, x-NH$_2$py can also function as a bidentate ligand via the nitrogen donor atoms of both the pyridine ring and the –NH$_2$ group, as reported for the catena-{M(μ_2-3-NH$_2$py)(H$_2$O)$_4$]SO$_4$·H$_2$O (M = Ni, Co) complex (Mautner *et al.*, 2021). Complex containing x-NH$_2$py ligands exhibit a wide diversity of structural motifs, ranging from molecular complexes such as [Zn(4-NH$_2$py)$_2$(SCN)$_2$] (Dasna *et al.*, 2023b), to dimeric complexes such as [Cd(2-NH$_2$py)$_3$(NCS)($\mu_{1,5}$-SCN)]$_2$ (Wijaya *et al.*, 2024), and polymeric structures such as [Ni(4-NH$_2$py)$_2$(NCS)$_2$]$_n$ (Neumann *et al.*, 2018). The presence of the –NH$_2$ group in the x-NH$_2$py ligand contributes to the formation of

Cite this as: Lestari, P. D., Farida, N., Wijaya, H. W., and Dasna, I. W. (2026). Synthesis, Characterization, Hirshfeld Surface Analysis, and Antibacterial Properties of Complex [Ni(4-aminopyridine)$_4$Cl$_2$].H$_2$O. *ALCHEMY Jurnal Penelitian Kimia*, 22(2), 492-503. doi: https://dx.doi.org/10.20961/alchemy.22.2.112417.492-503.

Copyright © 2026, Universitas Sebelas Maret, ISSN 1412-4092, e ISSN 2443-4183

three-dimensional architectures due to its ability to establish intermolecular interactions with neighboring molecules (Mariyam *et al.*, 2024).

Nickel(II) has been extensively studied due to its wide range of applications, including as an antibacterial agent (Rasyda *et al.*, 2021), anticancer agent (Li *et al.*, 2020), contrast agent (Olatunde *et al.*, 2012), catalyst (Wenger, 2021), and energy storage material (Karushev *et al.*, 2021). This metal is well known for its high flexibility in forming coordination bonds with a variety of ligands, both organic and inorganic, ranging from small to bulky ones (Sheikhshoaie *et al.*, 2018; Bazanov *et al.*, 2024). Ni(II) complexes are capable of adopting various geometries, including square planar (Lomjanský *et al.*, 2018), tetrahedral (Sarı *et al.*, 2013), trigonal bipyramidal (Marriott *et al.*, 2015), square pyramidal (Panigrahi *et al.*, 2022), and octahedral (Chakrabarty *et al.*, 2015). This structural diversity is attributed to the electronic configuration of Ni(II) (d^8), in which slight variations in the ligand field can induce changes in the molecular geometry (Chastanet *et al.*, 2018). Such geometric versatility leads to variations in the physicochemical properties, which in turn influence the biological activity of Ni(II) complexes and their interactions with bacterial cells.

Ni(II) ions have been reported to exhibit antimicrobial activity at low concentrations, suggesting potential oligodynamic behavior (Damena *et al.*, 2023). This is supported by the study of Al-Qadsy *et al.* (2023), which showed that the antibacterial activity of Ni(II) complexes increases significantly compared to their free ligands. Furthermore, the Ni(II) complexes exhibited lower MIC values than both the Zn(II) complexes and the free ligand. The Ni(II) complex exhibited MIC values in the range of 1.95 – 7.81 µg/mL, even surpassing the effectiveness of commonly used antibiotics such as streptomycin. The antibacterial mechanism of Ni(II) is suggested to be related to its ability to disrupt essential enzymatic functions through interactions with enzyme active sites. This is further supported by molecular docking studies, which revealed that the Ni(II) complex has a high binding affinity toward NAD synthetase from *Escherichia coli*, with a docking score of −7.61 kcal/mol, thereby inhibiting vital metabolic processes in bacteria and effectively leading to cell death.

Although Ni(II) ions exhibit antibacterial activity, their effectiveness is significantly enhanced upon complexation (Rasyda *et al.*, 2021). In their free form, Ni(II) ions are highly hydrophilic, which limits their ability to penetrate the lipid bilayer of bacterial cell membranes. Upon coordination with ligand donor atoms, the polarity of the metal ion is reduced as a result of partial sharing of its positive charge with the ligand's donor atom. This interaction facilitates electron delocalization within the complex, thereby enhancing its hydrophobic and lipophilic character. As a result, the complex can penetrate the bacterial cell membrane more efficiently, thereby enhancing its oligodynamic antibacterial activity (Colette *et al.*, 2014).

The complex $[Ni(3\text{-}NH_2py)_4Cl_2]$ has been synthesized and evaluated for its antibacterial activity; however, it exhibited low activity (Lestari *et al.*, 2025). Efforts to enhance antibacterial activity can be achieved through several approaches, one of which involves ligand modification by substituting 3-NH_2py with 4-NH_2py. The change in the amino group position from meta to para on the pyridine ring leads to a more delocalized electron distribution, thereby increasing the electron-donating ability of the ligand toward the central metal ion. This positional change also reduces steric repulsion around the pyridine nitrogen atom, resulting in a more stable coordination with the metal center (Orie *et al.*, 2021). The improved coordination stability enables the formation of Ni(II) complexes with more favorable electronic properties, which in turn enhance the interaction between the complex and bacterial cell membranes, leading to stronger antibacterial activity (Sharma *et al.*, 2022; Narita *et al.*, 2025). Several Ni(II) complexes with aminopyridine ligands have been synthesized and tested for their antibacterial activity, including $[Ni(C_5H_5N)_2Cl_2]$ (Islam *et al.*, 2015), $[Ni(3\text{-}NH_2py)_4Cl_2]$ (Lestari *et al.*, 2025), and $[Ni(2\text{-}NH_2py)_2(dca)_2]$ (Laksmana *et al.*, 2023).

Based on the discussion above it can be concluded that the combination of Ni(II) ions with N-heterocyclic ligands, such as aminopyridine, shows considerable promise for the development of coordination compounds with antibacterial activity. Consequently, the synthesis of the $[Ni(4\text{-}NH_2py)_4Cl_2]\cdot H_2O$ complex is of considerable interest, as it is anticipated to produce a structurally more stable complex with improved antibacterial activity.

RESEARCH METHODS

The materials used in this study included $NiCl_2\cdot 6H_2O$ (Merck, p.a. 98%), 4-aminopyridine (Merck Millipore, p.a. 98%), methanol (Merck Emsure®, p.a. 99%), distilled water, aluminum foil, plastic wrap, and Whatman filter paper No. 42. All chemicals were used without further purification.

The synthesis was carried out using the solvothermal method adapted from Dasna *et al.* (2023b), with modifications to the temperature and reaction time. A solution of 4-NH_2py (0.3765 g, 4 mmol) was prepared in 5

Copyright © 2026, Universitas Sebelas Maret, ISSN 1412-4092, e ISSN 2443-4183

mL of methanol. Then, a methanolic solution of $NiCl_2 \cdot 6H_2O$ (0.2377 g, 1 mmol) was slowly added to the 4-NH_2py solution. The mixture was stirred for 1 hour at room temperature, followed by solvothermal treatment at 68 °C for 15 hours. The mixture was filtered off, affording a light green precipitate and dark blue filtrate. The green precipitate was non-crystalline and was therefore not further characterized. Meanwhile, the filtrate was allowed to evaporate slowly until crystals were formed. Blue cubic crystals were obtained after 28 days of slow evaporation (yield = 32.80%).

Characterization of the complex included: (1) melting point analysis using a Fisher-John melting point apparatus within the range of 30 – 300 °C; (2) molar conductivity measurement using a Cyberscan CON 11/110 conductometer; (3) Infrared spectral analysis using a Shimadzu IRPrestige-21 spectrometer in KBr pellets within the range of 4000 – 400 cm^{-1}; (4) single-crystal X-ray diffraction (SC-XRD) data were collected at 296.(2) K using Bruker D8 Quest diffractometer with Mo Kα radiation (λ = 0.71073 Å), where data reduction and scaling were performed using the Bruker APEX 4 suite; and (5) Hirshfeld surface analysis using *Crystal Explorer* software. This analysis was used to visualize and quantify the intermolecular interactions within the complexes. The surfaces were mapped over d*norm*, shape index, and curvature surface. Fingerprint plots were also displayed over the range of 1.0 – 2.8 Å

The antibacterial activity test was carried out using the Kirby–Bauer disc diffusion method on Mueller–Hinton agar medium against *E. coli* (ATCC 25922) and *S. aureus* (ATCC 23235), with chloramphenicol as a positive control. The bacterial inoculum was prepared by suspending 4 – 5 colonies from a pure culture into 2 mL of sterile saline solution and adjusting the turbidity to match the 0.5 McFarland standard (1.5 × 10^8 CFU/mL). A sterile cotton swab was dipped into the bacterial suspension and evenly spread across the MH agar surface. The complex compound, metal salt, and ligand were dissolved in 10% DMSO at a concentration of 5 mg/mL. Discs were then placed on the agar surface, and the plates were incubated in an inverted position at 35 ± 2 °C for 24 hours. The inhibition zone diameters were measured in millimeters (Hudzicki, 2016).

RESULTS AND DISCUSSION

Synthesis of $[Ni(4\text{-}NH_2py)_4Cl_2]\cdot H_2O$ Complex

The complex $[Ni(4\text{-}NH_2py)_4Cl_2]\cdot H_2O$ was synthesized using the solvothermal method by reacting $NiCl_2 \cdot 6H_2O$ with 4-aminopyridine (4-NH_2py) in a 1:4 molar ratio in methanol solvent. The solvothermal process was carried out at 68 °C for 15 hours. Blue block-shaped crystals were obtained after slow evaporation for 28 days (yield = 32.80%). The chemical reaction equation for the formation of the complex is shown in Figure 1. The physical appearance of the synthesized complex differed from its reactants, indicating the successful formation of a new compound distinct from the starting materials (Figure 2) (Wijaya *et al.*, 2023).

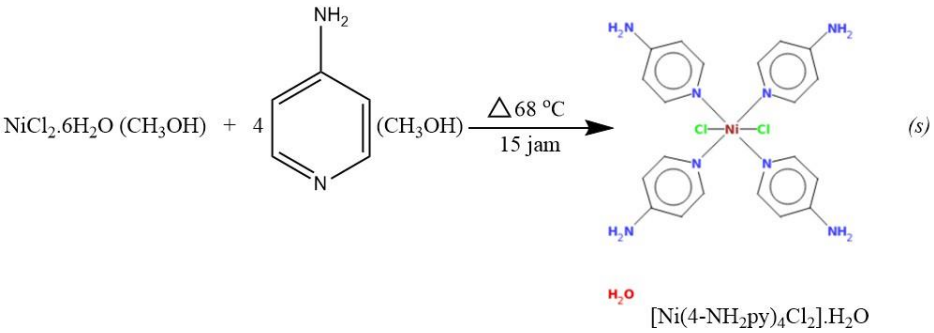

Figure 1. The chemical reaction equation for the formation of the complex $[Ni(4\text{-}NH_2py)_4Cl_2]\cdot H_2O$.

$NiCl_2 \cdot 6H_2O$ 4-NH_2py The synthesized crystal

Figure 2. The difference in the physical appearance of the complex compared to its reactants.

The synthesized complex decomposed at a temperature range of 225 – 230 °C, accompanied by a color change from blue to brown. The molar conductance value of the synthesized compound was 541 µS/cm, indicating

Copyright © 2026, Universitas Sebelas Maret, ISSN 1412-4092, e ISSN 2443-4183

that the compound behaves as an electrolyte. In aqueous solution, a compound is classified as a non-electrolyte if its molar conductance value is < 80 µS/cm and as an electrolyte if it is > 118 µS/cm. Based on this reference, the synthesized complex in aqueous medium can be categorized as an ionic complex.

FTIR Analysis

Based on the IR spectrum of the $[Ni(4\text{-}NH_2py)_4Cl_2]\cdot H_2O$ complex shown in Figure 3, an absorption band is observed at 3316 cm^{-1}, which is attributed to the symmetric stretching vibration of the $–NH_2$ group from the 4-NH_2py ligand. The asymmetric stretching vibration of the $–NH_2$ group, typically appearing around 3400 cm^{-1} is still detected but with very low intensity. This is likely due to the appearance of a broad new band at 3208 cm^{-1}, corresponding to the O–H stretching vibration (Ikemoto *et al.*, 2022). The breadth of this band causes overlap with the $–NH_2$ asymmetric stretching, resulting in the disappearance of the characteristic $–NH_2$ absorption band of the 4-NH_2py ligand.

Additionally, absorption bands at 1510 and 1277 cm^{-1} are attributed to the aromatic stretching vibrations of C=N and C–NH_2, which are characteristic of the pyridine ring of the 4-NH_2py ligand (Kartal and Şahin, 2021). The Ni–N coordination vibration appears in the fingerprint region at 553 cm^{-1} (Singh *et al.*, 2006; Alramadhan *et al.*, 2023). The observed blue shift in the ring-breathing mode indicates that coordination between the metal center and the 4-NH_2py ligand occurs through the pyridine nitrogen atom. The interaction between the donor N atom of the pyridine ring and the Ni(II) center leads to a partial decrease of electron density from the nitrogen lone pair, causing electron delocalization within the ring. This delocalization stabilizes the system and results in a blue shift in the FTIR spectrum (Buyukmurat and Akyuz, 2003).

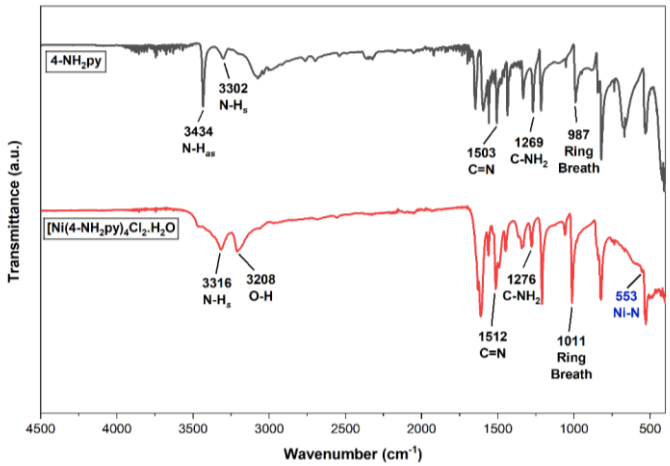

Figure 3. FTIR spectrum of the complex $[Ni(4\text{-}NH_2py)_4Cl_2]\cdot H_2O$ and its ligand.

Structural Analysis

The $[Ni(4\text{-}NH_2py)_4Cl_2]\cdot H_2O$ complex is a monomeric complex with a distorted octahedral geometry around the central Ni^{2+} ion. The complex is isostructural with $[Cu(4\text{-}NH_2py)_4Cl_2]\cdot H_2O$ H_2O (Fun *et al.*, 2008). The asymmetric unit consists of one Ni^{2+} center, four 4-NH_2py ligands, two chloride ions, and one water molecule (Figure 4). In this complex, the 4-NH_2py ligand coordinates in a monodentate manner through the pyridine nitrogen donor atom. Coordination bonds are formed between the Ni^{2+} ion and four pyridine nitrogen atoms from the 4-NH_2py ligands, along with two chloride ions. Meanwhile, one water molecule is located outside the coordination sphere. The complex crystallizes in the monoclinic crystal system with the space group $P2_1/n$. The crystallographic data of the complex are presented in Table 1.

The Ni–N bond lengths are in the range of 2.090(2) – 2.113(2) Å, while the Ni1–Cl1 and Ni1–Cl2 bond lengths are 2.5252(8) and 2.5319(8) Å, respectively (Table 2). Compared to its isostructural analogue $[Cu(4\text{-}NH_2py)_4Cl_2]\cdot H_2O$ (CCDC No. 696387), the Cu–N bond lengths are in the range of 2.0140(11) – 2.0258(11) Å, whereas the Cu1–Cl1 and Cu1–Cl2 bond lengths are 3.2185(4) and 2.7199(3) Å, respectively. Overall, the Ni–N bond lengths are slightly longer (by approximately ±0.07 – 0.09 Å), while the Ni–Cl bond lengths are shorter (by approximately ±0.69 and 0.19 Å) than the corresponding Cu–N and Cu–Cl bonds. This difference is attributed to the Jahn–Teller distortion in the $[Cu(4\text{-}NH_2py)_4Cl_2]\cdot H_2O$ complex, which leads to elongation of the Cu–Cl bonds

Copyright © 2026, Universitas Sebelas Maret, ISSN 1412-4092, e ISSN 2443-4183

(along the z-axis) and consequently shortens the Cu–N bonds. Meanwhile, the bond angles in both complexes do not show significant differences.

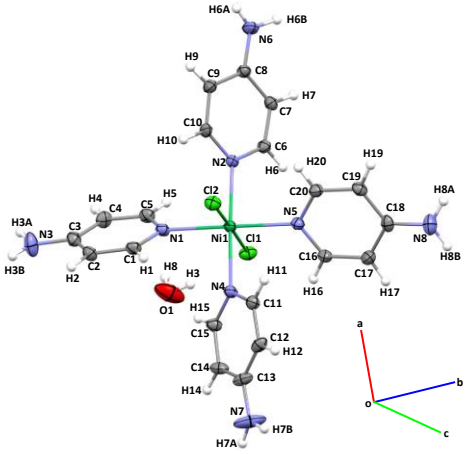

Figure 4. Structure of the $[Ni(4\text{-}NH_2py)_4Cl_2]\cdot H_2O$ complex.

Table 1. Crystallographic data of the $[Ni(4\text{-}NH_2py)_4Cl_2]\cdot H_2O$ complex.

Compound	**$[Ni(4\text{-}NH_2py)_4Cl_2]\cdot H_2O$**
CCDC No.	2428633
Empirical formula	$C_{20}H_{26}Cl_2N_8NiO$
Formula weight (g/mol)	524.10
Temperature (K)	296.(2)
Wavelength (Å)	0.71073
Crystal system	Monoclinic
Space group	$P2_1/n$
a (Å)	9.7665(4)
b (Å)	17.5841(7)
c (Å)	14.0100(6)
α (º)	90
β (º)	92.085(2)
γ (º)	90
V (Å^3)	2404.42(17)
Z	4
X-Ray radiation type	Mo Kα
Crystal size max/med/min (mm)	0.35/0.28/0.25
Absorption correction	Multi-Scan
Number of reflections	9466
F_{000}	1088
Density (g/cm^3)	1.448
Absorption coefficient (mm^{-1})	1.058
θ_{min} (°)	2.3868
θ_{max} (°)	28.2575
h, k, l_{max}	8, 23, 18
T_{min}, T_{max}	0.4836, 0.7457
Data/Parameters/Restraints	5929/289/0
R1 (1> 2σ(I))	0.0459
wR2	0.0874
Goodness of fit	1.197

The Ni–N bond lengths in this complex are shorter than in the $[Ni(3\text{-}NH_2py)_4Cl_2]$ complex, which range from 2.157(3) to 2.166(3) Å (Lestari *et al.*, 2025). This difference is influenced by the position of the –NH_2 group on the x-NH_2py ligand. In the $[Ni(4\text{-}NH_2py)_4Cl_2]\cdot H_2O$ complex, the –NH_2 group occupies the *para* position, whereas in the $[Ni(3\text{-}NH_2py)_4Cl_2]$ complex it is located at the *meta* position. The *para* position leads to a more symmetric complex with a smaller steric effect compared to the *meta* position. The greater steric repulsion in the complex

Copyright © 2026, Universitas Sebelas Maret, ISSN 1412-4092, e ISSN 2443-4183

with the 3-NH_2py ligand tends to elongate the Ni–N bonds beyond their ideal length, resulting in shorter Ni–N bonds in the [Ni(4-NH_2py)$_4$$Cl_2$]·$H_2O$ complex compared to those in [Ni(3-NH_2py)$_4$$Cl_2$].

The bond angles formed by donor atoms around the central Ni(II) ion also show deviations from the ideal octahedral angles (Table 3). These deviations result from steric effects that act to minimize ligand–ligand repulsion (Dasna *et al.*, 2023a). The N1–Ni1–Cl1 bond angle is 89.29(7)°, which is slightly smaller than the ideal value. The reduction of the angle corresponds to the orientation of the H_2O molecule within the crystal lattice, suggesting that the deviation is likely caused by interactions between the chloride ligand and the hydrogen atoms of the H_2O molecule, as further supported by the Hirshfeld surface analysis.

Table 2. Bond lengths around the central Ni(II).

Interatomic Bonds	Bond Lengths (Å)
Ni1-N1	2.113(2)
Ni1-N2	2.090(2)
Ni1-N4	2.105(2)
Ni1-N5	2.111(2)
Ni1-Cl1	2.5252(8)
Ni1-Cl2	2.5319(8)

Table 3. Bond angles around the central Ni(II).

Interatomic Angles	Bond Angles (°)
N2-Ni1-N4	177.24(9)
N2-Ni1-N5	89.14(9)
N4-Ni1-N5	88.23(9)
N2-Ni1-N1	90.63(9)
N4-Ni1-N1	92.03(9)
N5-Ni1-N1	177.94(9)
N2-Ni1-Cl1	91.49(7)
N4-Ni1-Cl1	89.30(7)
N5-Ni1-Cl1	88.66(7)
N1-Ni1-Cl1	89.29(7)
N2-Ni1-Cl2	91.09(7)
N4-Ni1-Cl2	88.09(7)
N5-Ni1-Cl2	90.77(7)
N1-Ni1-Cl2	91.28(7)
Cl1-Ni1-Cl2	177.35(3)

There are four complex molecules within one unit cell (Z = 4), as shown in Figure 5. The complex crystallizes in the $P2_1/n$ space group, which means that if one molecule in the crystal lattice is rotated by 180° about a plane perpendicular to the diagonal *n* axis and then translated by ½ along the *b* axis, an equivalent molecule will be obtained. Intermolecular hydrogen bonds are formed between the hydrogen atom of the NH_2 group on the 4-aminopyridine ligand and the oxygen atom of the water molecule (N8–H8A···O1, 1.975 Å). Additionally, further intermolecular interactions occur between the hydrogen atom of the water molecule and the chloride ion (H3···Cl1, 2.447 Å). Intermolecular interactions are indicated by blue dashed lines in Figure 6.

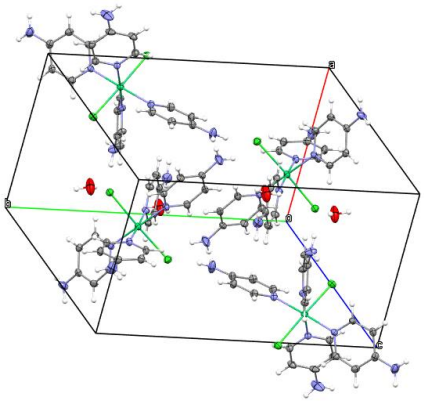

Figure 5. Arrangement of complex molecules in the crystal lattice.

Copyright © 2026, Universitas Sebelas Maret, ISSN 1412-4092, e ISSN 2443-4183

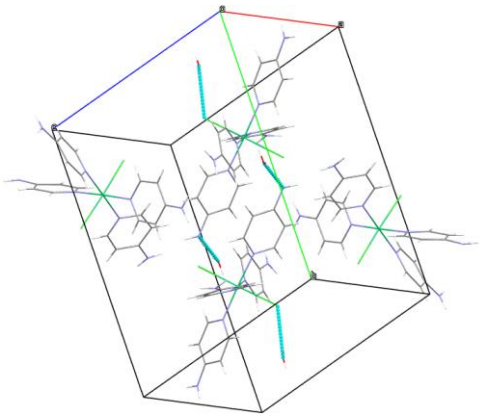

Figure 6. Intermolecular interactions of the complex compound $[Ni(4\text{-}NH_2py)_4Cl_2]\cdot H_2O$.

Hirshfeld Surface Analysis

Hirshfeld surface analysis was conducted to visualize and quantify the intermolecular interactions within the $[Ni(4\text{-}NH_2py)_4Cl_2]\cdot H_2O$ complex (Nasaruddin *et al.*, 2022). The d*norm* surface (Figure 7a) reveals that the presence of H_2O molecules in the crystal lattice plays a dominant role in the overall intermolecular interactions. The intense red spots around the hydrogen atoms of the $–NH_2$ groups in the 4-aminopyridine ligands indicate significant N–H···Cl and H···O hydrogen-bonding interactions with the chloride ligands and the oxygen atoms of the H_2O molecules, respectively. Similarly, red regions surrounding the Cl^- ligands confirm Cl···H contacts involving hydrogen atoms from both the $–NH_2$ groups and the coordinated water molecule.

The shape index map (Figure 7b) shows red areas around the Cl^- ligands involved in intermolecular interactions, suggesting their function as hydrogen-bond acceptors. In contrast, the blue regions around the hydrogen atoms of the $–NH_2$ groups demonstrate their function as hydrogen-bond donors. Meanwhile, the curvedness map (Figure 7c) displays extensive green regions representing flat molecular surfaces and blue areas corresponding to curved regions of the molecule. The blue curved regions are predominantly associated with H···H interactions, indicating H···H contacts significantly influence the molecular packing of the complex. Moreover, the flat green regions on the aromatic rings of the $4\text{-}NH_2py$ ligands suggest the presence of π···π stacking interactions contributing to the stabilization of the crystal structure.

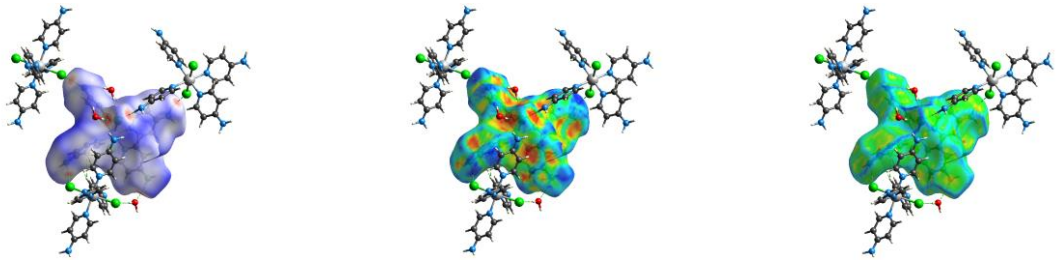

Figure 7. Hirshfeld surface analysis of the $[Ni(4\text{-}NH_2py)_4Cl_2]\cdot H_2O$ complex: (a) dnorm surface, (b) shape index, and (c) curvedness map.

The Hirshfeld surface fingerprint plot provides a comprehensive overview of intermolecular interactions within the crystal structure. The relative contributions of different contacts indicate the dominant interactions governing crystal packing (Spackman and Jayatilaka, 2009). Based on the fingerprint plot of the complex shown in Figure 8, the intermolecular contacts that contribute significantly to the crystal packing are H···H, C···H/H···C, H···Cl/Cl···H, and N···H/H···N, with respective contributions of 50.9%, 20.0%, 13.5%, and 9.0%. Other minor contacts contributing to the crystal packing include C···C and C···N/N···C interactions, accounting for 5.5% and 1.1%, respectively.

Copyright © 2026, Universitas Sebelas Maret, ISSN 1412-4092, e ISSN 2443-4183

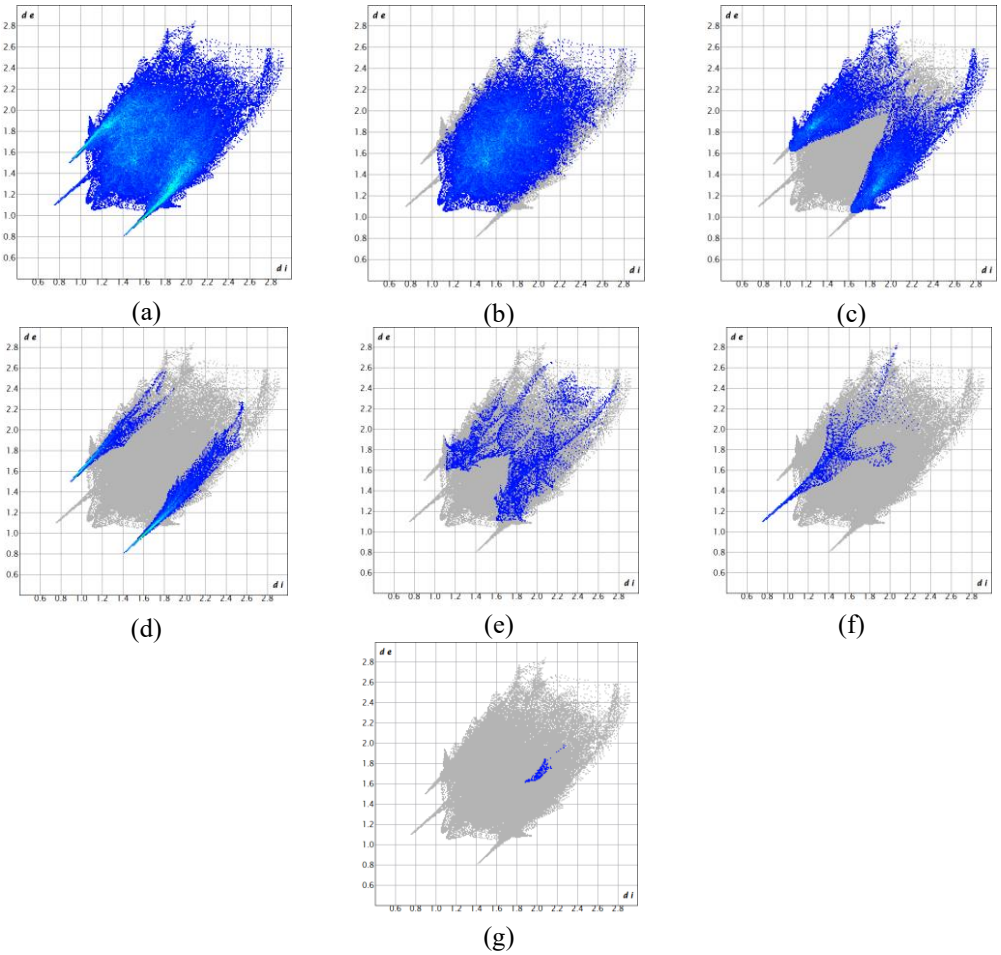

Figure 8. Fingerprint plot of the [Ni(4-NH$_2$py)$_4$Cl$_2$]·H$_2$O complex (a) Overall Interactions (100%), (b) H···H Interactions (53,3%), (c) C···H/H···C Interactions (26,5%), (d) H···Cl/Cl···H Interactions (11,4%), (e) N···H/H···N Interactions (6,1%), (f) H···O/O···H Interactions (2,4%), and (g) C···O/O···C Interactions (0,2%).

Antibacterial Properties

The antibacterial activity of the [Ni(4-NH$_2$py)$_4$Cl$_2$]·H$_2$O complex against *Staphylococcus aureus* (Gram-positive) and *Escherichia coli* (Gram-negative) was evaluated in vitro using the disc diffusion method (Kirby–Bauer) with 10% DMSO as the negative control and chloramphenicol as the positive control (Balouiri *et al.*, 2016). Chloramphenicol exhibited strong antibacterial activity against both bacteria, with inhibition zone diameters of 22.32 mm for *S. aureus* and 21.85 mm for *E. coli*. In contrast, the negative control (10% DMSO) showed no inhibition zones, indicating that the solvent itself has no antibacterial effect and does not affect the activity of the tested compounds. Compared to the positive control, the antibacterial activity of the tested complex was categorized as weak to moderate. These results suggest that the [Ni(4-NH$_2$py)$_4$Cl$_2$]·H$_2$O complex exhibits antibacterial potential, although its activity is still considerably lower than that of chloramphenicol. The detailed results are presented in Table 4.

The antibacterial activity of the [Ni(4-NH$_2$py)$_4$Cl$_2$]·H$_2$O complex was higher against *Escherichia coli* (Gram-negative) than against *Staphylococcus aureus* (Gram-positive), which can be attributed to differences in the cell wall structure between Gram-positive and Gram-negative bacteria. The structural differences are illustrated in Figure 9. The outer layer of the Gram-positive bacterial cell wall consists of a thick, polar peptidoglycan layer. In contrast, Gram-negative bacteria have an outer membrane coated with lipopolysaccharides, which are nonpolar, and also possess porins that serve as channels for passive transport of small molecules (Rohde, 2019). The complete antibacterial activity images are provided in Table S1.

The surface of the [Ni(4-NH$_2$py)$_4$Cl$_2$]·H$_2$O complex is dominated by four x-NH$_2$py ligands, which contain nonpolar carbon–carbon bonds within their aromatic rings. According to the principle of "like dissolves like," this relatively nonpolar complex can interact more easily with the nonpolar outer membrane of Gram-negative bacteria

Copyright © 2026, Universitas Sebelas Maret, ISSN 1412-4092, e ISSN 2443-4183

(Lübtow *et al.*, 2019). Furthermore, complexation can enhance the hydrophobic and lipophilic character of a compound by partially delocalizing the positive charge of the metal center onto the donor atoms of the ligands, allowing the complex to penetrate lipid-rich layers (lipopolysaccharides) more effectively and exhibit antibacterial activity (Colette *et al.*, 2014). These factors collectively explain why the $[Ni(4\text{-}NH_2py)_4Cl_2]\cdot H_2O$ complex exhibits higher antibacterial efficacy against Gram-negative bacteria compared to Gram-positive bacteria.

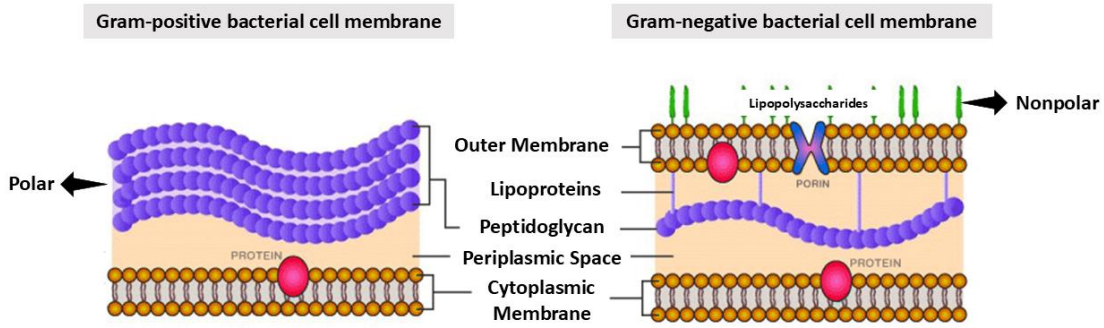

Figure 9. The difference between Gram-positive and Gram-negative bacterial membranes (adapted from Pimentel *et al.* (2022)).

Table 4. Antibacterial activity of complexes $[Ni(4\text{-}NH_2py)_4Cl_2]\cdot H_2O$ and their reactants.

No	Compound	Concentration (mg/mL)	Inhibition zone diameter (mm)	
			S. aureus	*E. coli*
1.	Chloramphenicol (+)	-	22.32	21.85
2.	DMSO 10% (-)	-	0.00	0.00
3.	$NiCl_2\cdot H_2O$	5	9.77	10.43
4.	$4\text{-}NH_2py$	5	6.55	11.60
5.	$[Ni(4\text{-}NH_2py)_4Cl_2]\cdot H_2O$	5	7.99	9.18

CONCLUSION

The complex $[Ni(4\text{-}NH_2py)_4Cl_2]\cdot H_2O$ was synthesized using solvothermal method in methanol at 68 °C for 15 h, affording blue cubic crystals (yield = 32.8%). Structural characterization showed a mononuclear complex with distorted octahedral geometry around Ni(II). Ni(II) coordinated by four nitrogen atoms from 4-aminopyridine ligands and two chloride ions, with an uncoordinated water molecule in the lattice. Hirshfeld surface analysis indicated that the crystal packing is primarily stabilized by N–H···Cl and H···O hydrogen-bonding interactions. Antibacterial activity tests showed that the complex exhibits greater inhibitory activity against *Escherichia coli* (Gram-negative) than *Staphylococcus aureus* (Gram-positive).

SUPPLEMENTARY INFORMATION

Table S1 is available in Supplementary Information and accessible at https://jurnal.uns.ac.id/alchemy/article/view/112417/supp.info.

CONFLICT OF INTEREST

The authors declare no conflict of interest. The funders had no role in the design of the study; in the collection, analysis, or interpretation of data; in the writing of the manuscript; or in the decision to publish the results.

AUTHOR CONTRIBUTION

PDL: Investigation, Data Analysis, Manuscript Drafting; IWD: Conceptualization, Supervision, Project Administration; NF: Supervision, Data Interpretation; HW: Manuscript Review and Editing.

ACKNOWLEDGEMENT

The authors gratefully acknowledge the financial support from Universitas Negeri Malang through the Institute of Research and Community Service (LPPM) under the PNBP Research Grant Scheme (Contract No. 24.2.664/UN32.14.1/LT/2025). The authors also express their gratitude to the Integrated Laboratory, Central

Copyright © 2026, Universitas Sebelas Maret, ISSN 1412-4092, e ISSN 2443-4183

Laboratory of Advanced Minerals and Materials, and Inorganic Chemistry Laboratory, Department of Chemistry, Universitas Negeri Malang, for providing laboratory facilities and technical assistance during this research.

DECLARATION OF GENERATIVE AI

No declaration of generative AI use was provided.

REFERENCES

Al-Qadsy, I., Saeed, W.S., Al-Owais, A.A., Semlali, A., Alrabie, A., Al-Faqeeh, L.a.S., Alsaeedy, M., Al-Adhreai, A., Al-Odayni, A.-B., and Farooqui, M., 2023. Antimicrobial Activity of Novel Ni(II) and Zn(II) Complexes with (E)-2-((5-Bromothiazol-2-Yl)Imino)Methyl)Phenol Ligand: Synthesis, Characterization and Molecular Docking Studies. *Antibiotics* 12, 1634. https://doi.org/10.3390/antibiotics12111634.

Alramadhan, S.A., Hammud, H.H., Ali, B.F., Ghabbour, H.A., Sarfaraz, S., and Ayub, K., 2023. Structures, Characterization and DFT Studies of Four Novel Nickel Phenanthroline Complexes. *Crystals*, 13, 738. https://doi.org/10.3390/cryst13050738.

Amin, A., Qadir, T., Sharma, P.K., Jeelani, I., and Abe, H., 2022. A Review on the Medicinal and Industrial Applications of N-Containing Heterocycles. *The Open Medicinal Chemistry Journal*, 16, e187410452209010. https://doi.org/10.2174/18741045-v16-e2209010.

Balouiri, M., Sadiki, M., and Ibnsouda, S.K., 2016. Methods for In Vitro Evaluating Antimicrobial Activity: A Review. *Journal of Pharmaceutical Analysis*, 6, 71–79. https://doi.org/10.1016/j.jpha.2015.11.005.

Bazanov, D.R., Korolyov, E.D., Lyssenko, K.A., and Lozinskaya, N.A., 2024. Octahedral Oxo-Bridged Tri-Nickel(II) Complex with 1,3,5-Tris(2-Hydroxyphenyl)-2,4-Diazapenta-1,3-Diene. *Molbank*, M1945. https://doi.org/10.3390/M1945.

Buyukmurat, Y., and Akyuz, S., 2003. Theoretical and Experimental Studies of IR Spectra of 4-Aminopyridine Metal(II) Complexes. *Journal of Molecular Structure*, 651–653, 533–539. https://doi.org/10.1016/S0022-2860(02)00674-9.

Chakrabarty, M., Ahmed, A., and Lal, R.A., 2015. Synthesis, Characterization, and Structural Assessment of Ni(II) Complexes Derived from Bis(2-Hydroxy-1-Naphthaldehyde)Succinoyldihydrazone. *International Journal of Inorganic Chemistry*, 1–11. https://doi.org/10.1155/2015/121895.

Chastanet, G., Lorenc, M., Bertoni, R., and Desplanches, C., 2018. Light-Induced Spin Crossover—Solution and Solid-State Processes. *Comptes Rendus. Chimie*, 21, 1075–1094. https://doi.org/10.1016/j.crci.2018.02.011.

Colette, A., Ondoh, A.M., Yufanyi, D.M., and Yanick Gaelle, D.S., 2014. Synthesis, Crystal Structure and Antimicrobial Properties of an Anhydrous Copper(II) Complex of Pyridine-2-Carboxylic Acid. *International Journal of Chemistry*, 7, p10. https://doi.org/10.5539/ijc.v7n1p10.

Damena, T., Demissie, T.B., Bitew Alem, M., Zeleke, D., and Desalegn, T., 2023. In Vitro Biological Activities of Novel Ni(II)-2-Chloroquinoline Derivative Complex: Synthesis, Characterization and Computational Studies. *Results in Chemistry*, 6, 101090. https://doi.org/10.1016/j.rechem.2023.101090.

Dasna, I.W., Mariyam, D., Wijaya, H.W., Arrozi, U.S.F., and Sugiarto, S., 2023a. Synthesis, Structural Determination and Antibacterial Properties of Zinc(II) Complexes Containing 4-Aminopyridine Ligands. *Indonesian Journal of Chemistry*, 23, 1108. https://doi.org/10.22146/ijc.82801.

Dasna, I.W., Wijaya, H.W., Setta Putra, F.I., Abdulloh, H., and Taufiq, A., 2023b. Highly Efficient Synthesis of Complex Bis-2,4-Dimethoxy-1,3,5-Triazapentadienemetal(II) (Metal = Cu, Ni) with Hirshfeld Surface Analysis. *Malaysian Journal of Fundamental and Applied Sciences*, 19, 447–459. https://doi.org/10.11113/mjfas.v19n3.3018.

Fun, H.-K., Sinthya, A., Jebas, S.R., and Devadasan, S., 2008. Tetrakis(4-aminopyridine-κ N^1)dichloridocopper(II) monohydrate. *Acta Crystallographica Section E Structure Reports Online*, 64, m853–m854. https://doi.org/10.1107/S1600536808015778.

Hudzicki, J., 2016. Kirby-Bauer Disk Diffusion Susceptibility Test Protocol. *ASM*.

Ikemoto, Y., Harada, Y., Tanaka, M., Nishimura, S.-N., Murakami, D., Kurahashi, N., Moriwaki, T., Yamazoe, K., Washizu, H., Ishii, Y., and Torii, H., 2022. Infrared Spectra and Hydrogen-Bond Configurations of Water Molecules at the Interface of Water-Insoluble Polymers under Humidified Conditions. *The Journal of Physical Chemistry B*, 126, 4143–4151. https://doi.org/10.1021/acs.jpcb.2c01702.

Islam, F., Hossain, M.A., Shah, N.M., Barua, H.T., Kabir, M.A., Khan, M.J., and Mullick, R., 2015. Synthesis, Characterization, and Antimicrobial Activity Studies of Ni(II) Complex with Pyridine as a Ligand. *Journal of Chemistry*, 525239. https://doi.org/10.1155/2015/525239.

Copyright © 2026, Universitas Sebelas Maret, ISSN 1412-4092, e ISSN 2443-4183

Ivanova, B.B., and Mayer-Figge, H., 2005. Crystal Structure and Solid State Ir-Ld Analysis of a Mononuclear Cu(II) Complex of 4-Aminopyridine. *Journal of Coordination Chemistry*, 58, 653–659. https://doi.org/10.1080/00958970412331336295.

Kartal, Z., and Şahin, O., 2021. The Synthesis of Heteroleptic Cyanometallate Aminopyridine Complexes and an Investigation into Their Structural Properties with Various Spectroscopic Methods. *Journal of Molecular Structure*, 1227, 129514. https://doi.org/10.1016/j.molstruc.2020.129514.

Karushev, M., Smirnova, E., and Chepurnaya, I., 2021. Nickel(II) Complex of N4 Schiff Base Ligand as a Building Block for a Conducting Metallopolymer with Multiple Redox States. *Molecules*, 26, 2646. https://doi.org/10.3390/molecules26092646.

Laksmana, S.D., Wijaya, H.W., and Dasna, I.W., 2023. Synthesis, Characterization, and Antimicrobial of [Ni(2-ampy)2(dca)2]. *Proceeding of The 4th International Conference on Life Science and Technology (ICoLiST)*, 2023.

Lestari, P.D., Farida, N., and Dasna, I.W., 2025. Synthesis, Structure, Hirshfeld Surface Analysis, and Antibacterial Activity of [Ni(3-NH_2Py)$_4$$Cl_2$] Complex (3-$NH_2$Py = 3-aminopyridine). *Jurnal Kimia Sains dan Aplikasi*, 28, 106–114. https://doi.org/10.14710/jksa.28.3.106-114.

Li, Y., Dong, J., Zhao, P., Hu, P., Yang, D., Gao, L., Li, L., and Pettinari, C., 2020. Synthesis of Amino Acid Schiff Base Nickel (II) Complexes as Potential Anticancer Drugs in Vitro. *Bioinorganic Chemistry and Applications*, 1–15. https://doi.org/10.1155/2020/8834859.

Lomjanský, D., Rajnák, C., Titiš, J., Moncoľ, J., Smolko, L., and Boča, R., 2018. Impact of Tetrahedral and Square Planar Geometry of Ni(II) Complexes with (Pseudo)Halide Ligands to Magnetic Properties. *Inorganica Chimica Acta*, 483, 352–358. https://doi.org/10.1016/j.ica.2018.08.029.

Lübtow, M.M., Haider, M.S., Kirsch, M., Klisch, S., and Luxenhofer, R., 2019. Like Dissolves Like? A Comprehensive Evaluation of Partial Solubility Parameters to Predict Polymer–Drug Compatibility in Ultrahigh Drug-Loaded Polymer Micelles. *Biomacromolecules*, 20, 3041–3056. https://doi.org/10.1021/acs.biomac.9b00618.

Mariyam, D., Dasna, I.W., Wijaya, H.W., and Danar, 2024. Synthesis, Characterization and Antibacterial Properties of Complex [Ag(Scn)(2-Nh2py)]. *E3S Web of Conferences*, 473, 03006. https://doi.org/10.1051/e3sconf/202447303006.

Marriott, K.E.R., Bhaskaran, L., Wilson, C., Medarde, M., Ochsenbein, S.T., Hill, S., and Murrie, M., 2015. Pushing the Limits of Magnetic Anisotropy in Trigonal Bipyramidal Ni(II). *Chemical Science*, 6, 6823–6828. https://doi.org/10.1039/C5SC02854J.

Mautner, F.A., Jantscher, P.V., Fischer, R.C., Torvisco, A., Reichmann, K., and Massoud, S.S., 2021. Syntheses, Structural Characterization, and Thermal Behaviour of Metal Complexes with 3-aminopyridine as Co-Ligands. *Transition Metal Chemistry*, 46, 191–200. https://doi.org/10.1007/s11243-020-00436-2.

Munadhiroh, A., Wijaya, H.W., Farida, N., Golhen, S., and Dasna, I.W., 2022. Synthesis, Characterization, and Preliminary Study of [Co(2- aminopyridine)2(NCS)2] or bis(2-aminopyridine)dithiocyanato Cobalt(II) as an Antibacterial. *Jurnal Kimia Valensi*, 8, 23–29. https://doi.org/10.15408/jkv.v8i1.22685.

Narita, M., Yamamoto, Y., Nakane, D., Akitsu, T., Pinlap, B.R., Pone Kamdem, B., and Fekam Boyom, F., 2025. Correlation between Calculated Electronic Properties and Antibacterial Activity of Chiral Amino Acid Schiff Base Copper(II) Complexes. *Discover Chemistry* 2, 185. https://doi.org/10.1007/s44371-025-00249-1.

Nasaruddin, N.H., Ahmad, S.N., Sirat, S.S., Tan, K.W., Zakaria, N.A., Mohamad Nazam, S.S., Rahman, N.M.M.A., Mohd Yusof, N.S., and Bahron, H., 2022. Synthesis, Structural Characterization, Hirshfeld Surface Analysis, and Antibacterial Study of Pd(II) and Ni(II) Schiff Base Complexes Derived from Aliphatic Diamine. *ACS Omega*, 7, 42809–42818. https://doi.org/10.1021/acsomega.2c04688.

Neumann, T., Ceglarska, M., Germann, L.S., Rams, M., Dinnebier, R.E., Suckert, S., Jess, I., and Näther, C., 2018. Structures, Thermodynamic Relations, and Magnetism of Stable and Metastable Ni(NCS)$_2$ Coordination Polymers. *Inorganic Chemistry*, 57, 3305–3314. https://doi.org/10.1021/acs.inorgchem.8b00092.

Olatunde, A.O., Dorazio, S.J., Spernyak, J.A., and Morrow, J.R., 2012. The Nicest Approach: Nickel(II) Paracest Mri Contrast Agents. *Journal of the American Chemical Society*, 134, 18503–18505. https://doi.org/10.1021/ja307909x.

Orie, K.J., Duru, R.U., and Ngochindo, R.I.O., 2021. Syntheses, Complexation and Biological Activity of Aminopyridines: A Mini-Review. *American Journal of Heterocyclic Chemistry*, 7, 11. https://doi.org/10.11648/j.ajhc.20210702.11.

Panigrahi, D., Mondal, M., Gupta, R., and Mani, G., 2022. Four- and Five-Coordinate Nickel(II) Complexes Bearing New Diphosphine–Phosphonite and Triphosphine–Phosphite Ligands: Catalysts for *N*-alkylation of Amines. *RSC Advances*, 12, 4510–4520. https://doi.org/10.1039/D1RA08961G.

Copyright © 2026, Universitas Sebelas Maret, ISSN 1412-4092, e ISSN 2443-4183

Pimentel, P.R.S., Brant, L.M.D.S., Lima, A.G.V.D.O., Cotrim, D.C., Nascimento, T., and Oliveira, R.L., 2022. How Can Nutritional Additives Modify Ruminant Nutrition? *Revista de la Facultad de Ciencias Agrarias UNCuyo*, 54, 175–189. https://doi.org/10.48162/rev.39.076.

Rasyda, Y.A., Widowati, M.K., Marliyana, S.D., and Rahardjo, S.B., 2021. Synthesis, Characterization and Antibacterial Properties of Nickel(II) Complex with 4-Aminoantipyrine Ligand. *Indonesian Journal of Chemistry*, 21, 391. https://doi.org/10.22146/ijc.56552.

Rohde, M., 2019. The Gram-Positive Bacterial Cell Wall. *Microbiology Spectrum*, 7, 7.3.10. https://doi.org/10.1128/microbiolspec.GPP3-0044-2018.

Sarı, N., Şahin, S.Ç., Öğütcü, H., Dede, Y., Yalcin, S., Altundaş, A., and Doğanay, K., 2013. Ni(II)-Tetrahedral Complexes: Characterization, Antimicrobial Properties, Theoretical Studies and a New Family of Charge-Transfer TransitionsYalçın. *Spectrochimica Acta Part A: Molecular and Biomolecular Spectroscopy*, 106, 60–67. https://doi.org/10.1016/j.saa.2012.12.078.

Sharma, B., Shukla, S., Rattan, R., Fatima, M., Goel, M., Bhat, M., Dutta, S., Ranjan, R.K., and Sharma, M., 2022. Antimicrobial Agents Based on Metal Complexes: Present Situation and Future Prospects. *International Journal of Biomaterials*, 1–21. https://doi.org/10.1155/2022/6819080.

Sheikhshoaie, I., Lotfi, N., Sieler, J., Krautscheid, H., and Khaleghi, M., 2018. Synthesis, Structures and Antimicrobial Activities of Nickel(II) and Zinc(II) Diaminomaleonitrile-Based Complexes. *Transition Metal Chemistry*, 43, 555–562. https://doi.org/10.1007/s11243-018-0241-5.

Singh, K., Barwa, M., and Tyagi, P., 2006. Synthesis, Characterization and Biological Studies of Co(II), Ni(II), Cu(II) and Zn(II) Complexes with Bidentate Schiff Bases Derived by Heterocyclic Ketone. *European Journal of Medicinal Chemistry*, 41, 147–153. https://doi.org/10.1016/j.ejmech.2005.06.006.

Spackman, M.A., and Jayatilaka, D., 2009. Hirshfeld Surface Analysis. *CrystEngComm*, 11, 19–32. https://doi.org/10.1039/B818330A.

Wenger, O.S., 2021. Photoactive Nickel Complexes in Cross-Coupling Catalysis. *Chemistry – A European Journal*, 27, 2270–2278. https://doi.org/10.1002/chem.202003974.

Wijaya, H.W., Danar, D., and Abiddin, Z., 2023. Synthesis, Structure, and Hirshfeld Surface Analysis of Tetrakis(N,N'-Diethylthiourea)Bis(Isothiocyanato)Nickel. *Indonesian Journal of Material Research*, 1, 74–83. https://doi.org/10.26554/ijmr.20231313.

Wijaya, H.W., Nugraha, G.C., Alfian, V.D., Arrozi, U.S.F., Sari, M.E.F., Laksmana, S.D., Putra, F.I.S., and Dasna, I.W., 2024. Synthesis, Structure, Hirshfeld Surface Analysis and Antibacterial Activities of [Cd(2-ampy)3(NCS)(M1,5-SCN)]2 and [Cd(4-ampy)2(M1,5-dca)2]N Complexes (2-ampy = 2-aminopyridine, 4-ampy = 4-Aminopyridine, NCS = Thiocyanate, dca = Dicyanamide). *Chemistry of Inorganic Materials*, 3, 100054. https://doi.org/10.1016/j.cinorg.2024.100054.

Copyright © 2026, Universitas Sebelas Maret, ISSN 1412-4092, e ISSN 2443-4183